Activation and Deactivation Rates of Recombinant $GABA_A$ Receptor Channels Are Dependent on α-Subunit Isoform

Annette M. Lavoie,*# Jessica J. Tingey,* Neil L. Harrison,¶ Dolan B. Pritchett,‖ and Roy E. Twyman*#§

*Program in Neuroscience, University of Utah, Salt Lake City, Utah; #Human Molecular Biology and Genetics Program, University of Utah, Salt Lake City, Utah; §Departments of Neurology and Pharmacology, University of Utah, Salt Lake City, Utah; ¶Departments of Anesthesia and Critical Care, and Pharmacological and Physiological Sciences, University of Chicago, Chicago, Illinois; and ‖Department of Pharmacology, University of Pennsylvania, Philadelphia, Pennsylvania, USA

ABSTRACT The role of subunit composition in determining intrinsic maximum activation and deactivation kinetics of $GABA_A$ receptor channels is unknown. We used rapid ligand application (100-μs solution exchange) to examine the effects of α-subunit composition on GABA-evoked activation and deactivation rates. HEK 293 cells were transfected with human cDNAs encoding $\alpha_1\beta_1\gamma_2$- or $\alpha_2\beta_1\gamma_2$-subunits. Channel kinetics were similar across different transfections of the same subunits and reproducible across several GABA applications in the same patch. Current rise to peak was at least twice as fast for $\alpha_2\beta_1\gamma_2$ receptors than for $\alpha_1\beta_1\gamma_2$ receptors (reflected in 10–90% rise times of 0.5 versus 1.0 ms, respectively), and deactivation was six to seven times slower (long time constants of 208 ms versus 31 ms) after saturating GABA applications. Thus α-subunit composition determined activation and deactivation kinetics of $GABA_A$ receptor channels and is therefore likely to influence the kinetics and efficacy of inhibitory postsynaptic currents.

INTRODUCTION

Native $GABA_A$ receptors may be composed of α-, β-, γ-, δ-, or ϵ-subunits (see Olsen and Tobin, 1990; Burt and Kamatchi, 1991; Whiting et al., 1995 for review, Davies et al., 1997). The classical benzodiazepine-sensitive $GABA_A$ receptor is thought to assemble as a heteropentamer containing 2α-, 2β-, and 1γ-subunits (for a review see Schofield, 1989, Chang et al., 1996); however, the particular isoform of each subunit that is expressed in individual neurons is dependent on anatomical location (Laurie et al., 1992; Wisden et al., 1992; Endo and Olsen, 1993; see Vicini, 1991 for review) and developmental stage (Mhatre and Ticku, 1992; Schlumpf et al., 1992; Fritschy et al., 1994; Gutierrez et al., 1994). Several different isoforms within each subunit class can be selectively expressed in nonneuronal cells. Certain isoforms and combinations of isoforms appear to contribute unique characteristics to $GABA_A$ receptor function. In combination with β- and/or γ-subunits, the α-subunit isoform can determine receptor binding affinity for GABA; specifically, α_2-containing receptors have reportedly demonstrated a 10-fold higher apparent GABA affinity than α_1-containing receptors in *Xenopus* oocytes (Levitan et al., 1988). β-Subunits at least contribute to the agonist binding site (Amin and Weiss, 1993) and may also control channel gating properties (Verdoorn et al., 1990). The inclusion of γ-subunits with α and β increases single-channel main-state conductance (Verdoorn et al., 1990; Angelotti and Macdonald, 1993). Furthermore, both α- and γ-subunits are involved in determining benzodiazepine agonist sensitivity (Pritchett et al., 1989; Kleingoor et al., 1991; Puia et al., 1991; Horne et al., 1993; Wafford et al., 1993; Ebert et al., 1994).

Although it is apparent that subunit composition of the $GABA_A$ receptor plays an important role in receptor pharmacology, many previous studies of receptor activation and deactivation properties have been technically limited by relatively slow presentation of ligand to the receptor (Sigel et al., 1990; Puia et al., 1991; Gingrich et al., 1995). The time course of neurotransmitter action at central synapses can be extremely brief (e.g., glutamate; Clements et al., 1992). Hence the mechanism by which these molecular processes relate to the function of these receptor channels under nonequilibrium conditions at the synapse remains uncertain. Rapid application techniques have been used to estimate the maximum activation rate of native cerebellar $GABA_A$ receptors at 6000 s^{-1} (Maconochie et al., 1994), but structural determinants of the opening rate have not been investigated. Subunit composition has been demonstrated to influence current decay, with longer time constants for $\alpha_3\beta_2\gamma_2$ versus $\alpha_1\beta_2\gamma_2$ receptors (Verdoorn et al., 1990; Verdoorn, 1993), but slower ligand applications have prevented resolution of maximum current onset. Rapid ligand application to multichannel patches now permits the resolution of both the activation and deactivation kinetics of $GABA_A$ receptors of defined subunit composition, as well as predictions concerning inhibitory synaptic function.

In this study we addressed the link between molecular composition and function of $GABA_A$ receptors by evaluating the dependence of $GABA_A$ receptor channel kinetic characteristics on the isoform of the α-subunit expressed. Using rapid ligand exchange techniques, we distinguished between two separate kinetic steps involved in receptor activation of recombinant receptors: ligand binding and channel gating. Furthermore, we measured current decay in

Received for publication 26 February 1997 and in final form 30 July 1997.

Address reprint requests to Dr. Roy E. Twyman, Eccles Institute of Human Genetics, University of Utah, Salt Lake City, UT 84112. Tel.: 801-585-6343; Fax: 801-585-3501; E-mail: roy.twyman@genetics.utah.edu.

0006-3495/97/11/2518/09 $2.00

the continued presence of ligand (current desensitization) or after its removal (current deactivation). This direct examination of the intrinsic kinetic properties of expressed receptor proteins revealed that α-subunit expression can regulate maximum activation and intrinsic deactivation rates of expressed $GABA_A$ receptor channels without affecting receptor desensitization kinetics. A more comprehensive understanding of the relationships between receptor structure and kinetic function utilizing this approach promises to lend insight into regional variations in GABAergic function and inhibitory postsynaptic current kinetics.

MATERIALS AND METHODS

Transformed human embryonic kidney (HEK 293) cells (ATCC CRL 1573) were plated onto 35-mm culture dishes in minimum essential medium (Sigma; with glutamine and glucose added) and 10% fetal calf serum and maintained in 5% CO_2. Standard Ca_2PO_4 precipitation techniques (Chen and Okayama, 1987) were used to transfect cells with plasmid (pCIS2; Pritchett et al., 1988) containing either human $\alpha_1\beta_1$ or $\alpha_2\beta_1$ and γ_2 cDNAs (2:1 ratio, 3 μg). Nontransfected cells did not demonstrate GABA-evoked currents and polymerase chain reaction analysis of nontransfected cells revealed no $GABA_A$ α, β, or γ transcripts (A. M. Lavoie et al., unpublished results).

At least 48 h after transfection, culture medium was exchanged for external salt solution (in mM: 142 NaCl, 1.5 KCl, 1 $CaCl_2$, 1 $MgCl_2$, 10 glucose, 30 sucrose, and 10 Na-HEPES at pH 7.4, adjusted to 320 mOsm with sucrose). Recording patch pipettes were filled with internal salt solution (in mM: 140 CsCl, 4 $MgCl_2$, 10 Na-HEPES, and 5 EGTA at pH 7.4, adjusted to 290 mOsm with H_2O). All experiments were carried out at a holding potential of −75 mV at room temperature (20–23°C).

A 1 M GABA (Sigma, St. Louis, MO) stock solution in distilled water was prepared before experiments and frozen in 1-ml aliquots. GABA dilutions (10 μM to 30 mM) were applied via gravity-assisted pressure ejection, using a rapid ligand exchange system. Excised outside-out multichannel patches (containing >10 channels) were placed into the stream of control external solution flowing from one side of a double-lumen thin-septum (theta) glass pipette. The theta tube apparatus was mounted on a piezoelectric transducer (Burleigh Instruments LSS-3100, with power supply PZ 150 amplifier/driver) that was software driven via pClamp6.0 (Axon Instruments) command potentials. Command potential onset and offset proceeded in a three-step ramp fashion (0.15-ms durations to 67%, 83%, and 100% full amplitude, 0.05 ms plateau, reverse to baseline) to minimize bounce. The duration of the command potential was varied according to experimental protocol (800-μs pulse; 50-ms to 2-s step). Activation of the piezoelectric transducer moved the interface between control and agonist solutions 40 μm laterally to rapidly expose the patch to GABA solutions (10 μM to 30 mM). Solution exchange time was determined to be ~100 μs by measuring the tip potential of an open electrode during exchange between salt solutions containing a >5% difference in NaCl osmolarity. Previously published reports have demonstrated similar rapid exchanges at an excised patch (2–2.5 times; Colquhoun et al., 1992; Maconochie et al., 1994). Data for which tip potentials did not conform to the command potential were discarded.

Recording micropipettes were constructed from borosilicate glass and had resistances of 3–5 MΩ. Currents from excised outside out multichannel patches were recorded with an Axopatch 200A amplifier (Axon Instruments) with an interposed eight-pole Bessel filter (low-pass 2–10 kHz; Frequency Devices). The filter bandwidth was chosen to maximize the resolution of current onset. Data were digitized at 10 times the filter bandwidth (20–100 kHz, pClamp 6.0 software; Axon Instruments) and simultaneously stored on a Digital audio tape (DAT; SONY 75ES digital audio tape deck modified to 0–20 kHz, 14-bit resolution, 44-kHz sampling frequency) and a strip chart recorder (Gould). Data were redigitized at lower rates when necessary to evaluate longer deactivation kinetics. Single-channel openings were recorded as above by using electrodes coated with Q-dope to reduce capacitance noise, and digitized at 2-kHz sampling frequency with a 2-kHz Bessel filter cutoff frequency. EC_{50} values were obtained by comparing normalized whole-cell peak current amplitudes in response to increasing GABA concentrations (300 nM to 10 mM). Available software (NFIT; Island Products, Galveston, TX) was used to find the optimal fit of the logistics equation to experimental dose-response curves.

Ensemble averages of sequential current responses of the same patch were obtained with software written by Dr. Twyman. Single application amplitudes ranged from ~20 to ~600 pA, depending on patch size, receptor density, and GABA concentration, so average current amplitudes were normalized to an arbitrary value of 100 to facilitate direct comparisons between patches harboring different numbers of receptors. The rise time was calculated as the time elapsed between 10% and 90% of the peak current amplitude. Data are reported as mean ± SEM. Multiexponential curve fitting of the patch current decay phase was performed with programs described previously (Twyman and Macdonald, 1992). Error ranges for the estimates were calculated by using maximum likelihood ranges ($m = 2$), which corresponded to a ~95% confidence interval. The number of significant exponential components was determined by fitting with increasing numbers of exponentials until the maximum likelihood estimate was no longer greatly improved by the inclusion of additional exponential components (LLR ≥ 4; McManus and Magleby, 1989; Twyman and Macdonald, 1992).

Single-channel current amplitudes and durations were determined by computer, using pClamp 6.0 (Axon Instruments) and software previously described (Macdonald et al., 1989; Twyman et al., 1990). Channel openings and closings were detected with the 50% threshold crossing method (based on 30-pS main state conductance). For the 2-kHz Bessel filter cutoff used in single-channel recording, openings were accepted as valid events if their durations were greater than twice the system rise time (340 μs), and closings were considered valid at durations greater than twice the system dead time (180 μs). Both openings and closings were collated into logarithmic frequency histograms (Sigworth and Sine, 1987; Twyman and Macdonald, 1992) for curve fitting of exponentials. A critical closed time for analytical determination of burst termination was obtained by using a modified method for minimization of misclassifications (Twyman et al., 1990). For $\alpha_2\beta_1\gamma_2$ and $\alpha_1\beta_1\gamma_2$ receptors, the critical closed times ("burst terminator") were 12 ms and 5 ms, respectively.

Macroscopic currents were modeled with available software (SCoP; Simulation Resources). Kinetic schemes were based on previous transient and steady-state kinetic models (Weiss and Magleby, 1989; Twyman et al., 1990; Maconochie et al., 1994; Jones and Westbrook, 1995; Lavoie and Twyman, 1996) and included two sequential binding sites, with multiple open and closed states. Models were fit to experimental data by using internal optimization functions that calculated the least-square error following variations in specific parameters.

RESULTS

Current activation rates

Net rates of channel activation are dependent upon both ligand concentration and binding affinity, as well as the time necessary for the protein conformational changes that are presumed to open the ion pore. To examine concentration-dependent activation rates for the $GABA_A$ receptor, we rapidly applied GABA in prolonged step applications for sufficient duration to allow the receptor-ligand interaction to reach equilibrium. Peak currents were normalized and receptor activation was measured as the time required for current onset to rise from 10% to 90% of peak current (10% to 90% rise time). Fig. 1 illustrates the GABA concentration-dependent current onset for $\alpha_1\beta_1\gamma_2$ and $\alpha_2\beta_1\gamma_2$ recep-

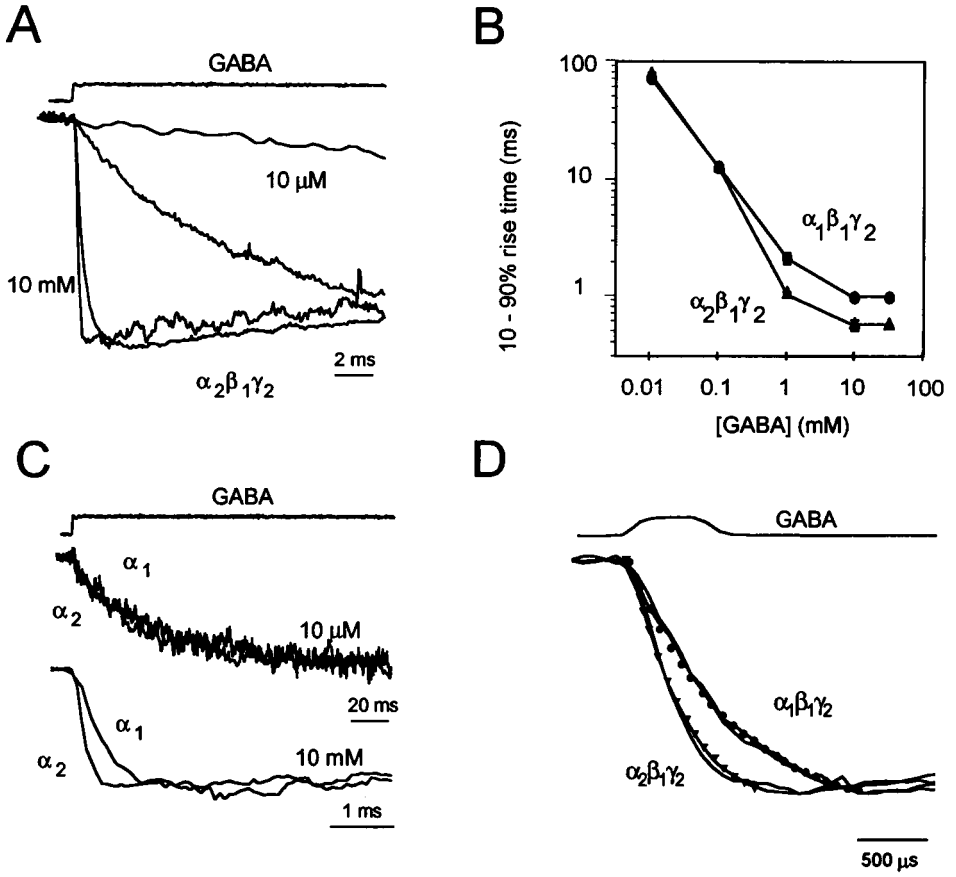

FIGURE 1 Channel activation kinetics are dependent upon GABA concentration and α-subunit composition. (*A*) Current activation for $\alpha_2\beta_1\gamma_2$ receptors after step (50 ms to 2 s) applications of 10 μM, 100 μM, 1 mM, and 10 mM GABA in different patches. Concentration-dependent responses were reproducible in the same patch and between patches. Responses represent ensemble averages of 10–40 GABA applications (20–600 pA peak current), which were normalized to the maximum peak current amplitude obtained in response to 10 mM GABA. (*B*) GABA concentration-dependent activation rates for $\alpha_1\beta_1\gamma_2$ and $\alpha_2\beta_1\gamma_2$ receptors after step applications of GABA. Log [GABA] is plotted against the time elapsed between 10% and 90% of peak current. Responses represent 8–10 applications for each receptor and demonstrated mean rise times for current onset of 72 ± 2.2, 12 ± 0.5, 2.1 ± 0.23, 1.0 ± 0.06, and 1.1 ± 0.03 ms for $\alpha_1\beta_1\gamma_2$ receptors (10 μM to 30 mM) and 77 ± 3.0, 12 ± 0.7, 1.0 ± 0.06, 0.5 ± 0.06, and 0.5 ± 0.02 ms for $\alpha_2\beta_1\gamma_2$ receptors. Both α_1- and α_2-containing receptor current amplitudes were saturated at 10 mM GABA. (*C*) Patch currents for $\alpha_1\beta_1\gamma_2$ and $\alpha_2\beta_1\gamma_2$ receptors after step applications (50 ms to 2 s) of 10 μM and 10 mM GABA. Responses represent ensemble averages of 10–40 traces (20–600 pA) and are normalized to peak current. (*D*) Activation rates were consistent across different cells and different transfections of the same subunits (150–600 pA peak amplitude) and are shown for two normalized pulse responses each for each receptor subtype. $\alpha_2\beta_1\gamma_2$ receptor current onset rise times to brief pulses of GABA were 0.6 ± 0.02 ms (fit τ = 2000 s^{-1}; ▼), whereas $\alpha_1\beta_1\gamma_2$ receptor current onset rise times were about twice as long at 1.0 ± 0.08 (fit τ = 3600 s^{-1}; ●).

tors ($n \geq 7$ for each GABA concentration, 10 μM to 30 mM). Application of low GABA concentrations (1 μM) demonstrated low efficiency of activation, making it difficult to resolve the 10% to 90% rise time. At the lowest GABA concentration analyzed (10 μM), current activation rates for α_1- and α_2-containing receptors were indistinguishable (Fig. 1 *C*; 10–90% rise time = 72 ± 2.2 (SEM) ms and 77 ± 3.0 ms, respectively; $p > 0.10$, $n \geq 7$). Progressive divergence between rates of current activation for α_1- and α_2-containing receptors was seen at higher GABA concentrations (Fig. 1 *B*; 100 μM, 12 ± 0.5 ms and 12 ± 0.7 ms, $p > 0.10$; 1 mM, 2.1 ± 0.23 ms and 1.0 ± 0.06 ms, respectively, $p < 0.01$). At saturating GABA concentrations (≥10 mM), $\alpha_2\beta_1\gamma_2$ receptor channels opened twice as fast, on average, as $\alpha_1\beta_1\gamma_2$ receptors (10 mM, 0.5 ± 0.06 ms and 1.0 ± 0.06 ms, respectively, $p < 0.001$, $n \geq 8$; 30 mM, 0.5 ± 0.02 ms and 1.1 ± 0.03 ms, $p < 0.001$, $n \geq 4$). Both receptor activation rise times were within the resolution of the application and recording system. However, if solution exchange at the patch were assumed to be up to three times greater than measured at the open electrode, the rise time for $\alpha_2\beta_1\gamma_2$ receptors could arguably approach the limits of our resolution. Regardless, the consistent and statistically significant difference between rise times for α_1- and α_2-containing receptors indicates that rise times are at least twofold different for the receptor subtypes. Current activation rates for both $\alpha_1\beta_1\gamma_2$ and $\alpha_2\beta_1\gamma_2$ receptors reached a plateau at 1–10 mM GABA concentrations, as evidenced by the log-log concentration-response plot (Fig. 1 *B*).

When the mean activation rates for each GABA concentration were fitted with the logistics equation, the EC_{50}

value for both $\alpha_1\beta_1\gamma_2$ and $\alpha_2\beta_1\gamma_2$ receptors was ~1 mM (1.0 and 1.3, respectively), compared with EC_{50} values for the peak amplitude of whole-cell recordings of 6.0 ± 1.9 μM and 37 ± 8.5 μM ($n \geq 5$; Hill number 1.2 and 1.8, respectively; data not shown). Maximum activation rates, estimated as the inverse of the best-fit single-exponential activation time constant (i.e., Maconochie et al., 1994), were around 2000 and 4200 s^{-1} (1960 ± 10 and 4240 ± 8) for $\alpha_1\beta_1\gamma_2$ and $\alpha_2\beta_1\gamma_2$ receptors, respectively, and were reproducible across transfection lots (Fig. 1 *D*). Measured 10–90% rise times were consistent with estimates of 80% peak current for these single-exponential time constants.

Current deactivation rates

For brief (<1 ms) pulses of agonist applied at 1.0–1.5-s intervals, decay phases of ensemble averages were fit with one to four time constants (Fig. 2). Decay currents for both $\alpha_1\beta_1\gamma_2$ and $\alpha_2\beta_1\gamma_2$ receptors were independent of GABA concentration and fit best with two exponentials. $\alpha_1\beta_1\gamma_2$ patch currents decayed with fast and slow time constants of 2.5 ± 0.4 and 31 ± 4.2 ms, and $\alpha_2\beta_1\gamma_2$ decayed with time constants of 21 ± 2.4 and 208 ± 5.0 ms. Currents recorded from patches containing $\alpha_2\beta_1\gamma_2$ receptors activated more quickly and decayed more slowly than those containing $\alpha_1\beta_1\gamma_2$ receptors. Because brief applications of GABA (<1 ms) essentially resulted in the synchronization of receptors in a bound state, current activation and deactivation kinetics after a pulse application of ligand represented the intrinsic maximum activation and deactivation rates of the receptor (Lavoie and Twyman, 1995).

Despite variability in the number of activated receptors in a patch, the current response profile also provided an estimate of the efficacy of charge transfer once the receptor was gated open. Both $\alpha_1\beta_1\gamma_2$ and $\alpha_2\beta_1\gamma_2$ receptors were shown to have similar single-channel main conductances, so normalization of peak current response to an arbitrary value permitted direct kinetic comparisons between patches containing different numbers of receptors. Integration of normalized peak current traces from onset to complete decay represented total charge transfer from synchronized and bound receptors and was thus used to compare efficiency between receptor populations independent of the number of channels activated. When peak currents were normalized, charge transfer after activation by a brief pulse of GABA was 10 times greater for $\alpha_2\beta_1\gamma_2$ receptors than for $\alpha_1\beta_1\gamma_2$ receptors. The longer decay time constant (31 and 208 ms) was responsible for 63 ± 7.3% and 95 ± 1.1% of the total area for $\alpha_1\beta_1\gamma_2$ and $\alpha_2\beta_1\gamma_2$ receptors, respectively.

Desensitization

Desensitization can be measured either as the decline in current during prolonged ligand application, or as a decrease in response amplitude to serial presentations of agonist. In contrast to deactivation, rates of current decay during prolonged applications (>50 ms) of 1 mM GABA were indistinguishable between patches containing $\alpha_1\beta_1\gamma_2$ and those containing $\alpha_2\beta_1\gamma_2$ receptors (Fig. 3). The decay phases of these currents were best fit with a single-exponential time constant of ~500 ms ($\alpha_1\beta_1\gamma_2$ 492 ± 128 and $\alpha_2\beta_1\gamma_2$ 449 ± 70; $n \geq 5$) and were considerably longer than the longest time constants measured for deactivation after agonist removal. Although desensitization has previously been reported to alter rates of receptor deactivation (Jones and Westbrook, 1995), these effects are minimized during brief pulse applications and therefore are not likely to be responsible for subunit specific differences in deactivation rates. Furthermore, serial applications of 1 mM GABA (<1-ms duration, 1–1.5-s intervals) did not demonstrate cumulative

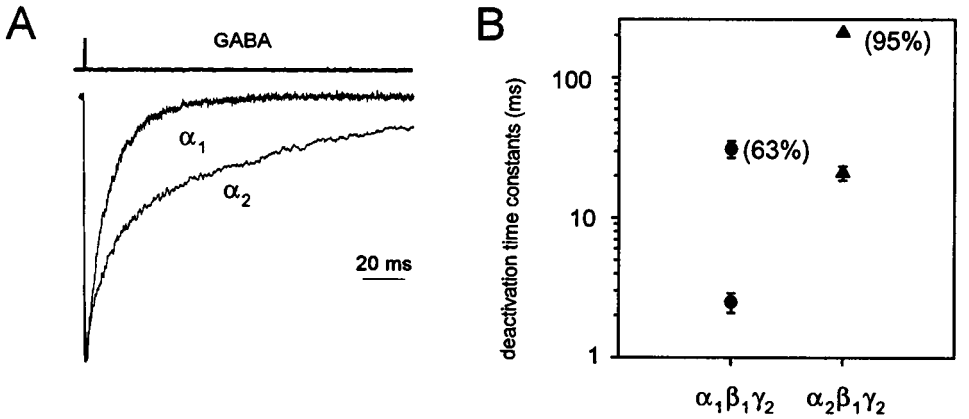

FIGURE 2 Deactivation kinetics are dependent upon α-subunit composition. (*A*) Pulse (<1 ms) applications of GABA yield patch currents with characteristic maximum activation rates and concentration-independent decay rates. Traces represent ensemble averages of 10 sequential GABA applications (10 mM; 150–600 pA peak current) and are normalized to peak current. Areas under the normalized responses were ~10 times greater for α_2- versus α_1-containing receptors. (*B*) Time constants of current decay after pulse application for both $\alpha_1\beta_1\gamma_2$ and $\alpha_2\beta_1\gamma_2$ receptors were fit best with two exponentials determined by the maximum log likelihood ratio method. The time constants for the fast components of decay were 2.5 ± 0.4 (SEM) ms and 21 ± 2.4 ms for α_1- and α_2-containing receptors, respectively, and the slow components were 31 ± 4.2 ms and 208 ± 5.0 ms, respectively ($n \geq 8$ each). The slow components contributed 63% and 95%, respectively, to the total current.

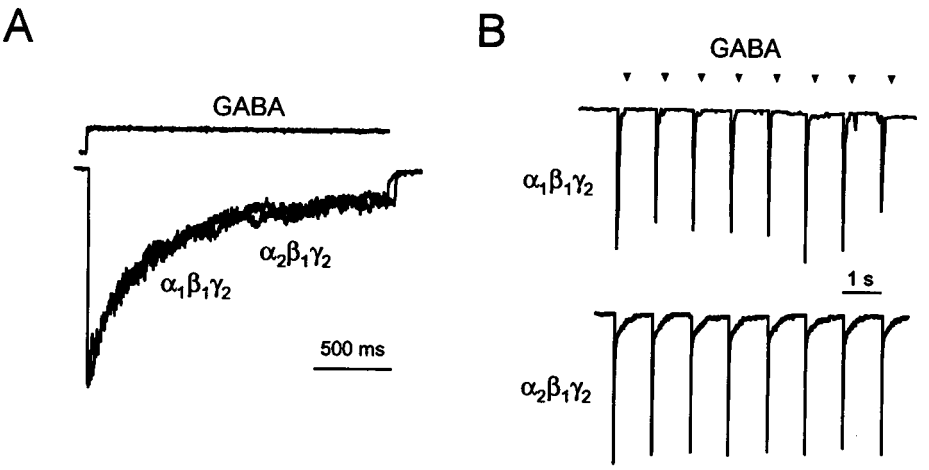

FIGURE 3 Desensitization characteristics during prolonged step applications of GABA are not dependent on α-subunit composition. (*A*) Current decay during a 2-s application of agonist was not different between patches containing $\alpha_1\beta_1\gamma_2$ or $\alpha_2\beta_1\gamma_2$ subunits ($n \geq 5$ patches for each subunit combination; peak currents 30–200 pA before normalization). Decay phases were fit best with a single exponential with a decay time constant of ~500 ms ($\alpha_1\beta_1\gamma_2$ 492 ± 128 and $\alpha_2\beta_1\gamma_2$ 449 ± 70). (*B*) Brief (<1 ms) pulses of agonist repeated at 1-s intervals resulted in no decrease in peak current amplitudes for either $\alpha_1\beta_1\gamma_2$ or $\alpha_2\beta_1\gamma_2$ receptors (60 and 120 pA, respectively).

desensitization in either α_1- or α_2-containing receptors. These results are consistent with previous reports that recombinant $GABA_A$ receptor desensitization is not dependent on α-subunit composition (Sigel et al., 1990; Verdoorn, 1993).

Single-channel parameters

To examine the single-channel properties associated with current decay of $\alpha_1\beta_1\gamma_2$ and $\alpha_2\beta_1\gamma_2$ receptors, single-channel openings were recorded after pulse applications of 1 mM GABA. Comparisons were made between the open, closed, and burst kinetics of $\alpha_1\beta_1\gamma_2$ and $\alpha_2\beta_1\gamma_2$ receptor channels. The single-channel main conductances of the two receptor types did not differ (30 ± 0.17 pS for $\alpha_1\beta_1\gamma_2$ and 30 ± 0.16 pS for $\alpha_2\beta_1\gamma_2$ receptors). Likewise, subconductances were similar for $\alpha_1\beta_1\gamma_2$ and $\alpha_2\beta_1\gamma_2$ receptor channels (19.4 ± 1.62 pS and 19.3 ± 0.47 pS, respectively), but subconductance openings contributed less than 5% of total current for each receptor type. The prominent single-channel kinetic differences between the recombinant receptor types were the prolonged open duration and bursting activity of $\alpha_2\beta_1\gamma_2$ receptors (Fig. 4). The main state conductance of α_2-containing receptors opened for a mean duration of 10.7 ms (2332 openings), with a mean burst duration (all bursts, containing one or more openings) of 85 ms (7.3 openings per burst) and a mean complex burst duration (bursts containing >2 openings) of 203 ms (13.5 openings per burst, 11.4-ms mean open duration). However, α_1-containing receptors demonstrated a 4.4-ms mean open duration (2736 openings), a mean burst duration of 17 ms (3.3 openings per burst), and a mean complex burst duration of 37 ms (6.6 openings per burst, 4.8-ms mean open duration). Complex bursts containing >2 openings are likely to represent the activity of fully liganded receptors (Twyman et al., 1990) and comprised 96% and 82% of all bursts for $\alpha_2\beta_1\gamma_2$ and $\alpha_1\beta_1\gamma_2$, receptors, respectively. These single-channel bursting properties are consistent with the time constants for macroscopic current deactivation (208 ms, 95% total current $\alpha_2\beta_1\gamma_2$; 31 ms, 63% total current $\alpha_1\beta_1\gamma_2$).

DISCUSSION

These results suggest that α-subunits are at least partially responsible for determining the gating kinetics of recombinant $GABA_A$ receptors. Activation rates for recombinant receptors were indistinguishable after prolonged applications of low GABA concentrations, but were at least twice as fast for $\alpha_2\beta_1\gamma_2$ receptors at saturating GABA concentrations. Furthermore, $\alpha_2\beta_1\gamma_2$ receptors demonstrated six to seven times slower relaxation kinetics than $\alpha_1\beta_1\gamma_2$ receptors. Together, these results suggest a mechanism for α-subunit-specific ligand-binding affinities and a role for subunit isoform variation at the central inhibitory synapse, where postsynaptic receptors may be exposed to GABA transiently and at high concentration (Maconochie et al., 1994; Jones and Westbrook, 1995).

A simple sequential binding model for the $GABA_A$ receptor

Rates of ligand binding and unbinding are integral determinants of the activation and deactivation currents of ligand-gated receptors; until recently, however, the separate events of binding and gating involved in receptor activation could not be distinguished. Receptors composed of $\alpha_2\beta_1\gamma_2$-subunits produced peak whole-cell GABA currents with a sixfold lower EC_{50} for GABA, relative to $\alpha_1\beta_1\gamma_2$ receptors when expressed in HEK 293 cells (data not shown; similar unpublished results were seen by V. V. Koltchine and N. L. Harrison, personal communication). The increased sensitivity to GABA for $\alpha_2\beta_1\gamma_2$ receptors may be interpreted as an increased affinity for GABA or in terms of an increased efficacy of GABA at $\alpha_2\beta_1\gamma_2$ receptors compared to $\alpha_1\beta_1\gamma_2$ receptors. However, the GABA concentration that elicited 50% of the maximum activation rate was similar for $\alpha_2\beta_1\gamma_2$

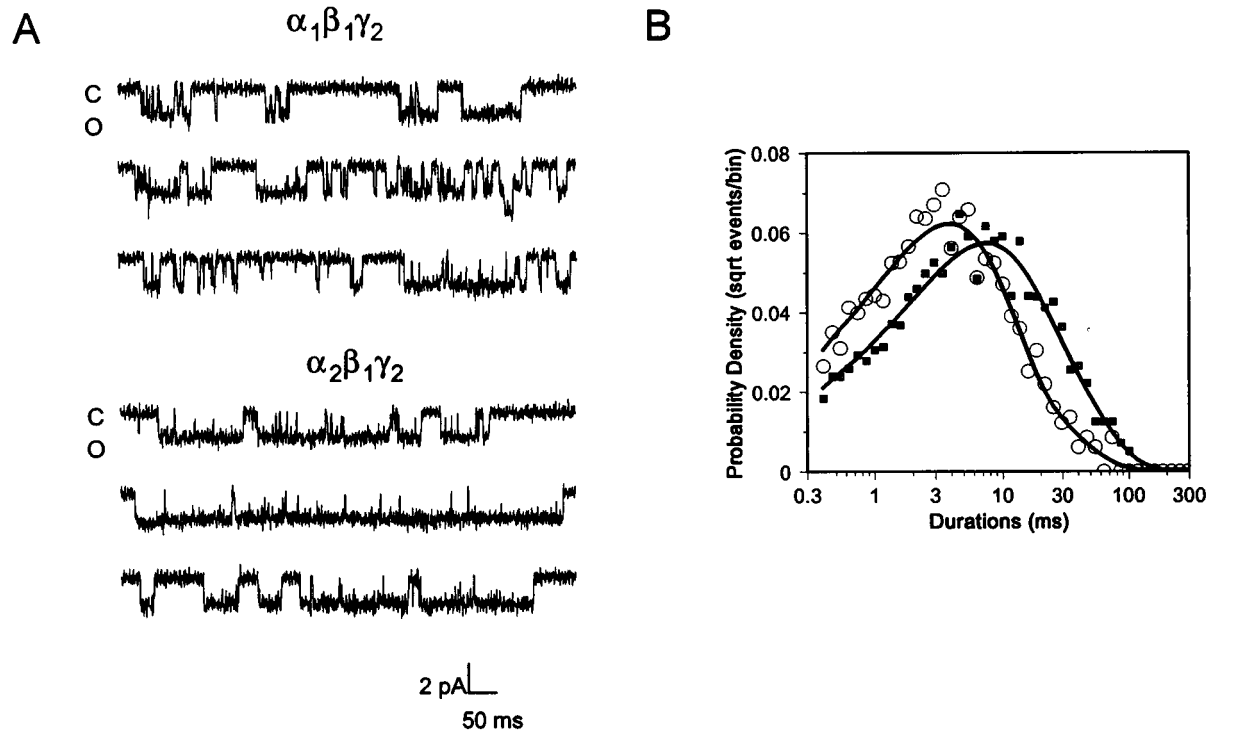

FIGURE 4 Single-channel burst characteristics are determined by α-subunit composition. (*A*) Oscillations between kinetic states as evidenced by changes in single-channel conductance, where C = closed states ($g \approx 0$) and O = open states ($g \approx 30$ pS). Nonconsecutive single-channel current traces from excised outside-out patches during 1 mM applications of GABA are shown to detail the typical burst behavior of each receptor type. Open and burst durations of $\alpha_2\beta_1\gamma_2$ were longer than those for $\alpha_1\beta_1\gamma_2$ receptors. (*B*) Probability density functions for single-channel open durations during 1 mM GABA applications demonstrate different kinetic properties of $\alpha_1\beta_1\gamma_2$ (○) and $\alpha_2\beta_1\gamma_2$ (■) receptors. Probability densities, representing the square root of the number of events per bin with 15 bins/decade, were best fit by two time constants ($\alpha_1\beta_1\gamma_2$: τ_1 = 4.0 ms −0.49 + 0.53, relative area 0.92; τ_2 = 11.8 ms −3.70 +5.45; $\alpha_2\beta_1\gamma_2$: τ_1 = 6.9 ms −1.17 + 1.38, relative area 0.70; τ_2 = 16.1 ms −2.78 + 3.19).

and $\alpha_1\beta_1\gamma_2$ receptors (~1 mM each), and higher than whole-cell EC_{50} values (6 and 37 μM, respectively). This difference between macropatch activation rate and peak whole-cell current EC_{50} values is similar to that previously reported (~100-fold; Maconochie et al., 1994) and reflects the differences in equilibrium versus dynamic effects of GABA on receptor response. For example, equilibrium peak responses were likely influenced more by desensitization and rapidly deactivating currents than dynamic responses, in a concentration-dependent manner.

Using rapid ligand exchange techniques and single-channel recording, the discrete events underlying binding affinity and efficacy can be examined in detail. For example, increases in binding affinity would be reflected in an increase in association and/or a decrease in dissociation rates for GABA. Alternatively, changes in receptor efficacy might be detected as alterations in the single-channel burst kinetics, because of differences in transitions between fully liganded open and closed states for the two receptor subtypes. Current molecular kinetic models indicate that native $GABA_A$ receptor channel gating is complex, with at least two GABA binding sites, three open states, and several possible desensitized states (Weiss and Magleby, 1989; Twyman et al., 1992; Jones and Westbrook, 1995). However, a simple sequential binding linear model can be used initially to understand the kinetic distinction between binding and gating events in recombinant channels after brief exposure to GABA.

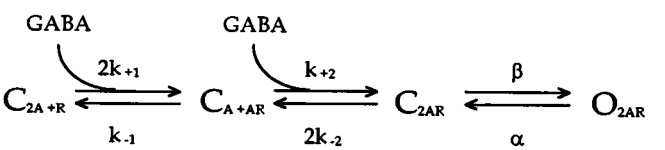

In this simple model, current onset at saturating GABA concentrations would be primarily exponentially shaped and described by the sum of α + β rates (where $\beta \gg \alpha$). Although more complex desensitizing models may better predict native responses under equilibrium conditions, the effects of desensitization on activation and/or deactivation kinetics are minimized by brief agonist applications (Jones and Westbrook, 1995). Saturating concentrations of GABA evoke current responses, with maximum rates of activation primarily determined by the gating rate of the channel and virtually independent of ligand binding factors, provided that ligand is applied faster than the time required for conformational changes to open the receptor. At saturating GABA concentrations, the 10–90% rise time for $\alpha_2\beta_1\gamma_2$

receptors was at least twice as fast as that for $\alpha_1\beta_1\gamma_2$ receptors, illustrating an intrinsic structural dependence of opening rate. Net activation rates after prolonged applications of low GABA concentrations are primarily determined by the rates of GABA binding. If the difference in binding affinity between $\alpha_1\beta_1\gamma_2$ and $\alpha_2\beta_1\gamma_2$ receptors were due to dissimilarity in the association rate constants for GABA binding (k_{+1}, k_{+2}), then differences in the time course of current onset would be expected between the two receptor populations during application of low agonist concentrations to steady state. Instead, rates of activation were nearly indistinguishable for $\alpha_1\beta_1\gamma_2$ and $\alpha_2\beta_1\gamma_2$ receptors after application of lower GABA concentrations, indicating that the microscopic association rates k_{+1} and k_{+2} must not be greatly different between the two receptors.

Current activation kinetics

An estimate of the GABA association rate constants k_{+1} and k_{+2} can be obtained by comparing the current onset at different GABA concentrations. For both $\alpha_2\beta_1\gamma_2$ and $\alpha_1\beta_1\gamma_2$ receptors, kinetic profiles of the current onset at low concentrations of GABA were indistinguishable, whereas differences at high GABA concentrations were significant. Using the simple model above, simulated current onsets were fit to experimental concentration-dependent current onsets by minimizing the least-squares error. Estimated in this way, k_{+2} is thought to be on the order of $4-5 \times 10^7$ M^{-1} s^{-1} for both receptor subtypes. Estimates of k_{+1} for $\alpha_1\beta_1\gamma_2$ and $\alpha_2\beta_1\gamma_2$ receptors fixed this k_{D2} value in the model and allowed k_{+1} to vary, resulting in rates on the order of 10^6 M^{-1} s^{-1} for both receptor subtypes. The binding events thus appear to be positively cooperative in this sequential binding model.

At saturating GABA concentrations, α_2-containing receptors opened at least twice as fast as α_1-containing receptors, and thus ($\beta + \alpha$) was at least twice as great for $\alpha_2\beta_1\gamma_2$ versus $\alpha_1\beta_1\gamma_2$ receptors. If β is equal to or greater than k_{-2}, the channel will be more likely to reopen, resulting in bursts of two or more openings separated by longer closed dwell times. A higher ratio of β/k_{-2} or a longer average open duration ($1/\alpha$) would yield a more prolonged current decay, the time constant of which would be closely approximated by the mean single-channel burst duration. Because the single-channel data indicate that the open channel exhibits bursting behavior (13.5 and 6.6 openings per complex burst for α_2- and α_1-containing receptors, respectively), and because α is relatively small (93 and 220 s^{-1}, respectively), the reopening rate β must be several times greater than k_{-2}. The average number of openings per burst for $\alpha_2\beta_1\gamma_2$ receptors is about twice that found for $\alpha_1\beta_1\gamma_2$ receptors. If β were to remain constant, a reduction of k_{-2} by 50% would result in an approximate doubling of the mean openings per burst. However, because β is much greater than k_{-2}, a 50% reduction in k_{-2} would not produce the 50% reduction in the lifetime in C_{2AR} observed for α_2-containing receptors. Taken together, the twofold increase in the maximum opening rate of $\alpha_2\beta_1\gamma_2$ receptors must be the result of an approximate doubling of the reopening rate constant β relative to $\alpha_1\beta_1\gamma_2$ receptors. This conclusion is consistent with the data comparing estimates of maximum activation rates between the two receptor types. The maximum opening rate ($\alpha + \beta$) for $\alpha_2\beta_1\gamma_2$ receptors (calculated as (10–90% rise time/2.2)$^{-1}$, where 2.2 is the time constant to traverse 80% current amplitude) was ~4400 s^{-1}, resulting in an estimate of $\beta \approx 4300$ s^{-1}. This was approximately twice the estimate for $\alpha_1\beta_1\gamma_2$ receptors (~2000 s^{-1}), indicating that α-subunit composition is at least partially responsible for the maximum opening rate.

Current deactivation kinetics

According to the simple gating model outlined above, current relaxation after agonist removal is determined by the relative rate constants for channel closing (α), opening (β), and ligand unbinding (k_{-2}). On removal of GABA, $\alpha_2\beta_1\gamma_2$ receptors relaxed considerably more slowly than did $\alpha_1\beta_1\gamma_2$ receptors. Single-channel recordings demonstrated that this slower current decay was due to the longer average open duration and increased likelihood of bursting, resulting in a considerably longer average burst duration for $\alpha_2\beta_1\gamma_2$ receptors. The fivefold increase in burst duration approximates the six- to sevenfold increase in the long decay time constant found for $\alpha_2\beta_1\gamma_2$ receptors compared to $\alpha_1\beta_1\gamma_2$ receptors. This long time constant was responsible for the majority of the area under the current decay for both recombinant receptor types and approximated the complex burst durations seen in the single-channel recordings. Thus current decay after GABA application results from the fully liganded receptor exiting from bursting states.

Using the simple model described above for a pulse application (<1 ms) of GABA, relaxation of the receptor from a fully bound conformation provides an estimate of the unbinding rate, which can be determined from the lifetime in C_{2AR} and the number of openings per burst predicted by this model ($= 1 + \beta/k_{-2}$). The result reveals that the estimated k_{-2} for both receptor types is approximately the same order of magnitude (~350 s^{-1}) and β is estimated to be ~4300 s^{-1} and 2000 s^{-1} for $\alpha_2\beta_1\gamma_2$ and $\alpha_2\beta_1\gamma_2$ receptors, respectively. These estimates of k_{-2} are simple approximations, as the gating of the $GABA_A$ receptor is considerably more complex than that described by the simple model proposed above (Weiss and Magleby, 1989; Twyman et al., 1990, 1992).

Current response reproducibility

Because subunit composition determined rates of channel activation and decay, reproducibility of population responses to maximally activating ligand applications was useful as an indicator of consistent subunit expression and

composition in patches. Patches containing receptors comprising different subunit stoichiometries would likely yield different activation and decay kinetics. Comparison of the activation rates between patches from different cells transfected with a particular subunit combination yielded consistent current activation rates and profiles after brief applications (<1 ms) at saturating concentrations of GABA (Fig. 1 *D*), as well as reproducible rates and profiles for current decay (data not shown). These characteristic activation and decay kinetics likely indicate consistent subunit composition across receptor populations from different cells and different transfection days. Although these results suggest kinetic characteristics can be used to phenotype receptor subtypes, kinetic rates have previously been shown to be susceptible to modulation (Moss et al., 1992).

CONCLUSION

Kinetics of current activation and deactivation of GABA-evoked responses in recombinant $GABA_A$ receptors are dependent on subunit composition. Receptors containing $\alpha_2\beta_1\gamma_2$ subunits open at least twice as fast, and the resulting currents decay six to seven times slower than those generated by α_1-containing receptors. The 6- to 10-fold higher potency observed for α_2-containing receptors compared with α_1-containing receptors is due primarily to the increased efficacy of GABA at α_2-containing receptors once GABA has been bound. This increased efficacy is primarily due to a twofold increase in reopening rates of bound receptors and an increase in average open duration. These two mechanisms in concert result in longer bursts of channel activity that are responsible for the prolonged deactivation of $\alpha_2\beta_1\gamma_2$ receptors compared to $\alpha_1\beta_1\gamma_2$ receptors. These results suggest that native $GABA_A$ receptors that contain α_2 subunits are likely to induce IPSCs with significantly longer duration, and thus function more effectively to limit action potential generation, than receptors containing α_1-subunits.

We thank Dr. Matt Jones for his assistance with the initial pilot experiments, and Qing Ye and Suzanne Finn for technical assistance throughout the project.

Supported by a University of Utah Graduate Fellowship Award to AML, by National Institutes of Health NIGMS grants GM45129 and GM 00623 to NLH, and by grant NS31519 to RET.

REFERENCES

Amin, J., and D. S. Weiss. 1993. $GABA_A$ receptor needs two homologous domains of the β-subunit for activation by GABA but not by pentobarbital. *Nature.* 366:565–569.

Angelotti, T. P., and R. L. Macdonald. 1993. Assembly of $GABA_A$ receptor subunits: $\alpha_1\beta_1$ and $\alpha_1\beta_1\gamma_{2\sigma}$ subunits produce unique ion channels with dissimilar single-channel properties. *J. Neurosci.* 13: 1429–1440.

Burt, D. R., and G. L. Kamatchi. 1991. $GABA_A$ receptor subtypes: from pharmacology to molecular biology. *FASEB J.* 5:2916–2923.

Chang, Y., R. Wang, S. Barot, and D. S. Weiss. 1996. Stoichiometry of a recombinant $GABA_A$ receptor. *J. Neurosci.* 16:5415–5424.

Chen, C., and H. Okayama. 1987. High-efficiency transformation of mammalian cells by plasmid DNA. *Mol. Cell. Biol.* 7:2745–2752.

Clements, J. D., R. A. Lester, G. Tong, C. E. Jahr, and G. L. Westbrook. 1992. The time course of glutamate in the synaptic cleft. *Science.* 258:1498–1501.

Colquhoun, D., P. Jonas, and B. Sakmann. 1992. Action of brief pulses of glutamate on AMPA/kainate receptors in patches from different neurones of rat hippocampal slices. *J. Physiol. (Lond.).* 458:261–287.

Davies, P. A., M. C. Hanna, T. G. Hales, and E. F. Kirkness. 1997. Insensitivity to anaesthetic agents conferred by a class of $GABA_A$ receptor subunit. *Nature.* 385:820–823.

Ebert, B., K. A. Wafford, P. J. Whiting, P. Krogsgaard-Larsen, and J. A. Kemp. 1994. Molecular pharmacology of γ-aminobutyric acid type A receptor agonists and partial agonists in oocytes injected with different α, β, and γ, receptor subunit combinations. *Mol. Pharmacol.* 46: 957–963.

Endo, S., and R. W. Olsen. 1993. Antibodies specific for α-subunit subtypes of $GABA_A$ receptors reveal brain regional heterogeneity. *J. Neurochem.* 60:1388–1398.

Fritschy, J-M., J. Paysan, A. Enna, and H. Mohler. 1994. Switch in the expression of rat $GABA_A$-receptor subtypes during postnatal development: an immunohistochemical study. *J. Neurosci.* 14: 5302–5324.

Gingrich, K. J., W. A. Roberts, and R. S. Kass. 1995. Dependence of the $GABA_A$ receptor gating kinetics on the α subunit isoform; implications for structure-function relations and synaptic transmission. *J. Physiol. (Lond.).* 489:529–543.

Gutierrez, A., Z. U. Khan, S. J. Morris, and A. L. De-Blas. 1994. Age-related decrease of $GABA_A$ receptor subunits and glutamic acid decarboxylase in the rat inferior colliculus. *J. Neurosci.* 14:7469–7477.

Horne, A. L., P. C. Harkness, K. L. Hadingham, P. J. Whiting, and J. A. Kemp. 1993. The influence of the γ_{2L} subunit on the modulation of responses to $GABA_A$ receptor activation. *Br. J. Pharmacol.* 108: 711–716.

Jones, M. V., and G. L. Westbrook. 1995. Desensitized states prolong $GABA_A$ channel responses to brief agonist pulses. *Neuron.* 15:181–191.

Kleingoor, C., M. Ewert, G. von Blankenfeld, P. H. Seeburg, and H. Kettenmann. 1991. Inverse but not full benzodiazepine agonists modulate recombinant $\alpha_6\beta_2\gamma_2$ $GABA_A$ receptors in transfected human embryonic kidney 293 cells. *Neurosci. Lett.* 130:169–172.

Laurie, D. J., W. Wisden, and P. H. Seeburg. 1992. The distribution of thirteen $GABA_A$ receptor subunit mRNAs in the rat brain. III. Embryonic and postnatal development. *J. Neurosci.* 12:4151–4172.

Lavoie, A. M., and R. E. Twyman. 1995. The receptor channel system response: rapid "fingerprinting" of native and expressed $GABA_A$ receptors. *Soc. Neurosci. Abstr.* 21:848.

Lavoie, A. M., and R. E. Twyman. 1996. Direct evidence for diazepam modulation of $GABA_A$ receptor microscopic affinity. *Neuropharmacology.* 35:1383–1392.

Levitan, E. S., P. R. Schofield, D. R. Burt, L. M. Rhee, W. Wisden, M. Kohler, N. Fujits, H. F. Rodriguez, F. A. Stephenson, M. G. Darlison, E. A. Barnard, and P. H. Seeburg. 1988. Structural and functional basis for $GABA_A$ receptor heterogeneity. *Nature.* 335:76–79.

Macdonald, R. L., C. J. Rogers, and R. E. Twyman. 1989. Kinetic properties of the $GABA_A$ receptor main conductance state of mouse spinal cord neurones in culture. *J. Physiol. (Lond.).* 420:479–499.

Maconochie, D. J., J. M. Zempel, and J. H. Steinbach. 1994. How quickly can $GABA_A$ receptors open? *Neuron.* 12:61–71.

McManus, O. B., and K. L. Magleby. 1989. Kinetic time constants independent of previous single-channel activity suggest Markov gating for a large conductance Ca-activated K-channel. *J. Gen. Physiol.* 94: 1037–1070.

Mhatre, M. C., and M. K. Ticku. 1992. Aging related alterations in $GABA_A$ receptor subunit mRNA levels in Fischer rats. *Brain Res. Mol. Brain Res.* 14:71–78.

Moss, S. J., T. G. Smart, C. D. Blackstone, and R. L. Huganir. 1992. Functional modulation of $GABA_A$ receptors by cAMP dependent protein phosphorylation. *Science.* 257:661–665.

Olsen, R. W., and A. J. Tobin. 1990. Molecular biology of $GABA_A$ receptors. *FASEB J.* 4:1469–1480.

Pritchett, D. B., H. Sontheimer, C. A. Gorman, H. Kettenmann, P. H. Seeburg, and P. R. Schofield. 1988. Transient expression shows ligand gating and allosteric potentiation of $GABA_A$ receptor subunits. *Science.* 242:1306–1308.

Pritchett, D. B., H. Sontheimer, B. Shivers, S. Ymer, H. Kettenmann, P. R. Schofield, and P. H. Seeburg. 1989. Importance of a novel $GABA_A$ receptor subunit for benzodiazepine pharmacology. *Nature.* 338: 582–585.

Puia, G., S. Vicini, P. H. Seeburg, and E. Costa. 1991. Influence of recombinant γ-aminobutyric acid-$_A$ receptor subunit composition on the action of allosteric modulators of γ-aminobutyric acid-$_A$-gated Cl^- currents. *Mol. Pharmacol.* 39:691–696.

Schlumpf, M., R. Parmar, A. Schrieber, H. R. Ramseier, E. Butikofer, H. Abriel, M. Barth, T. Rhyner, and W. Lichtensteiger. 1992. Nervous and immune systems as targets for developmental effects of benzodiazepines. A review of recent studies. *Dev. Pharmacol. Ther.* 18:145–158.

Schofield, P. R. 1989. The $GABA_A$ receptor: molecular biology reveals a complex picture. *Trends Pharmacol. Sci.* 10:476–478.

Sigel, E., R. Baur, G. Trube, H. Mohler, and P. Malherbe. 1990. The effect of subunit composition of rat brain $GABA_A$ receptors on channel function. *Neuron.* 5:703–711.

Sigworth, F. J., and S. M. Sine. 1987. Data transformations for improved display and fitting of single-channel dwell time histograms. *Biophys. J.* 52:1047–1054.

Twyman, R. E., R. M. Green, and R. L. Macdonald. 1992. Kinetics of open channel block by penicillin of single $GABA_A$ receptor channels from mouse spinal cord neurones in culture. *J. Physiol. (Lond.).* 445:97–127.

Twyman, R. E., and R. L. Macdonald. 1992. Neurosteriod regulation of $GABA_A$ receptor single-channel kinetic properties of mouse spinal cord neurons in culture. *J. Physiol. (Lond.).* 456:215–245.

Twyman, R. E., C. J. Rogers, and R. L. Macdonald. 1990. Intraburst kinetic properties of the $GABA_A$ receptor main conductance state of mouse spinal cord neurones in culture. *J. Physiol. (Lond.).* 423:193–220.

Verdoorn, T. A. 1993. Formation of heteromeric γ-aminobutyric acid type A receptors containing two different α subunits. *Mol. Pharmacol.* 45: 475–480.

Verdoorn, T. A., A. Draguhn, S. Ymer, P. H. Seeburg, and B. Sakmann. 1990. Functional properties of recombinant rat $GABA_A$ receptors depend upon subunit composition. *Neuron.* 4:919–928.

Vicini, S. 1991. Pharmacologic significance of the structural heterogeneity of the $GABA_A$ receptor-chloride ion channel complex. *Neuropsychopharmacology.* 4:9–15.

Wafford, K. A., P. J. Whiting, and J. A. Kemp. 1993. Differences in affinity and efficacy of benzodiazepine receptor ligands at recombinant γ-aminobutyric $acid_A$ receptor subtypes. *Mol. Pharmacol.* 43:240–244.

Weiss, D. S., and K. L. Magleby. 1989. Gating scheme for single GABA-activated Cl-channel determined from stability plots, dwell-time distributions, and adjacent-interval durations. *J. Neurosci.* 9:1314–1324.

Whiting, P. J., R. M. McKernan, and K. A. Wafford. 1995. Structure and pharmacology of vertebrate $GABA_A$ receptor subtypes. *Int. Rev. Neurobiol.* 38:95–139.

Wisden, W., D. J. Laurie, H. Monyer, and P.H. Seeburg. 1992. The distribution of 13 $GABA_A$ receptor subunit mRNAs in the rat brain. I. Telencephalon, diencephalon, mesencephalon. *J. Neurosci.* 12: 1040–1062.